



Research paper

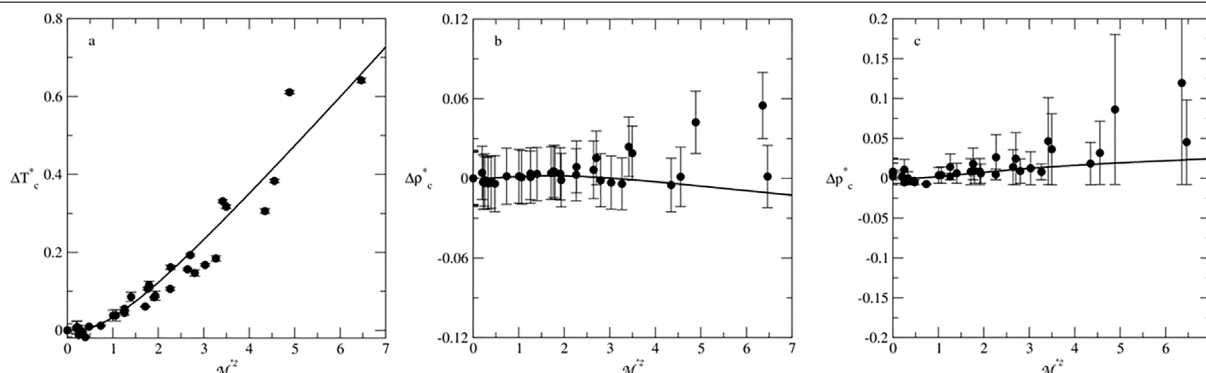
Thermodynamics of multipolar Kihara fluids. Results from Monte Carlo simulations and molecular discrete perturbation theory

Víctor M. Trejos^a, Francisco Gámez^{b,*}

^a Instituto de Ciencias Básicas e Ingeniería, Universidad Autónoma del Estado de Hidalgo, Carretera Pachuca-Tulancingo Km. 4.5, Col. Carboneras, C.P. 42184, Mineral de la Reforma, Hidalgo, Mexico

^b Department of Physical Chemistry, Universidad Complutense de Madrid, Madrid, Spain

GRAPHICAL ABSTRACT



HIGHLIGHTS

- Vapor–liquid equilibria of molecular fluids are affected by multipoles and geometry.
- Molecular discrete perturbation theory agrees with simulation results.
- The presence of dipole and quadrupole enhance individual effects on thermodynamics.

ARTICLE INFO

Keywords:

Multipolar fluids
Equation of state
Vapor–liquid equilibrium
Gibbs ensemble Monte Carlo

ABSTRACT

We present a systematic study of the vapor–liquid equilibria of prolate Kihara fluids embedding both dipole and quadrupole moments Monte Carlo simulations and perturbation theory methods. The agreement between both approaches is good and allows to shed light on some general features of molecular models whose distribution of charge can be modeled as a dipole plus a quadrupole moments. The validation of the equation of state does lead as a byproduct to a rapid, uncommon, and powerful instrument able to widen the frontiers of perturbation theory for molecular fluids and their mixtures.

1. Introduction

The thermodynamics of molecular models such as the ellipsoidal Gay–Berne [1,2], spherocylindrical Kihara [3–5], or chain-like multi-center Lennard-Jones [6–9] fluids have been widely explored in the

literature for decades. From those publications, it is well established that non-sphericity induced deviation from the corresponding states principle (CSP) [10]. The shape of the distribution of charge turns out to be another source of anisotropy that also cause deviations from the

* Corresponding author.

E-mail addresses: victor_trejos@uaeh.edu.mx (V.M. Trejos), frgamez@ucm.es (F. Gámez).

<https://doi.org/10.1016/j.cplett.2022.140171>

Received 26 July 2022; Received in revised form 5 October 2022; Accepted 31 October 2022

Available online 4 November 2022

0009-2614/© 2022 The Author(s). Published by Elsevier B.V. This is an open access article under the CC BY-NC-ND license (<http://creativecommons.org/licenses/by-nc-nd/4.0/>).

CSP [11,12]. Nevertheless, while molecular anisotropy tends to narrow the vapor–liquid density and lessen the critical properties, multipolar moments widen the orthobaric density profile and increase the critical temperature.

However, while thermodynamic properties of dipolar and quadrupolar atomic fluids have been widely explored in the literature with both simulation and theoretical methods [13–24] the exploration of models embedding both dipole and quadrupole moments have received considerably less attention [25–27]. If results dealing with the crossed dipole–quadrupole contribution are comparably much more scarce [25, 26] even harder to find are those works facing the combined effects on the thermodynamics induced by multipolar moments in elongated models. This is surprising since in the nature non-spherical multipolar molecules are much more the rule than the exception [28], so the study of coarse-grained models for these fluids pose an important information source for applied sciences [29]. In this context, the group of J. Vrabec focused their interest in nonpolar and polar two-centers Lennard-Jones models [30–32]. In relation with Kihara models, the group of S. Lago published a nice sequence of papers in which both the nonpolar [10,33–35] and the multipolar [10,11,24,27,36,37] spherocylindrical Kihara models were extensively studied with Boublik perturbation theory [38,39] and both Monte Carlo (MC) and Molecular Dynamics methods, even with the incorporation of subtle effects such as those coming from asymmetric and non-axial dipole moments [40]. In none of these interesting examples a systematic survey on the dipole–quadrupole interactions were assessed, a task that is accomplished in this work. Simulation data extracted by the Monte Carlo methods were used to validate a recently developed extended discrete perturbation theory (DPT) [18,41–46] for molecular and/or multipolar fluids as Kihara, Lennard-Jones dumbbells or square-well chains in both three- and two-dimensional systems (henceforth mol-DPT) [47–49]. Within this approach, an arbitrarily shaped potential can be mimicked with a sequence of square-shoulders (SS) and square-well (SW) steps whose energy well and width are effectively dependent on the molecular and multipolar anisotropy [47]. The theory was tested against reported data coming from Monte Carlo simulations for a wide ensemble of molecular fluids, but the dipole–quadrupole interactions were not incorporated into the validated model set. Here, we filled this gap by corroborating the theoretical results against new simulation data for a plethora of multipolar molecular fluids.

This work is organized into four sections. In Section 2, the Gibbs ensemble Monte Carlo (GEMC) simulation details and DPT used to describe the thermodynamic properties of multipolar fluids are presented. Then, in Section 3, a set of results concerning the vapor–liquid coexistence, vapor–pressure and critical properties are described in detail for a set of spherocylindrical Kihara fluids with dipole and quadrupole moments. Finally, some conclusions and perspectives are given in Section 4.

2. Methods

2.1. Model

In the present work, we consider a one-component system of multipolar prolate spherocylindrical Kihara fluid. In this model, the molecular shape is represented by a parallel body comprised of a linear core length L and a size parameter σ (width), with $L^* = L/\sigma$ the dimensionless length and with embedding both point dipole moment, μ , and quadrupole moment, Q . The molecular volume is then $v_m = (\pi\sigma^3/6)(1 + 1.5L^*)$.

The potential profile of a Kihara model has a Lennard-Jones feature, but the relevant intermolecular distance is the minimum distance between molecular cores (ρ) that depends on the mutual orientation and the center-to-center distance between the particles. Molecular cores are chosen to capture the main geometrical features of real molecules [50].

Hence, in this model the spherocylinders interact with each other through a potential given by:

$$u(r_{12}, \omega_1, \omega_2) = u^K(r_{12}, \omega_1, \omega_2) + u^{\mu\mu}(r_{12}, \omega_1, \omega_2) + u^{QQ}(r_{12}, \omega_1, \omega_2) + u^{\mu Q}(r_{12}, \omega_1, \omega_2), \quad (2.1)$$

where $r_{12} = |\mathbf{r}_{12}|$ is the distance between the center of mass of the molecules and $\omega_i \equiv \{\theta_i, \phi_i\}$ are the polar and azimuthal angles of each linear molecule's with respect to \mathbf{r}_{12} , respectively. In this equation, $u^K(r_{12}, \omega_1, \omega_2)$ is the Kihara potential [50], $u^{\mu\mu}(r_{12}, \omega_1, \omega_2)$ is the dipole–dipole potential [51], $u^{QQ}(r_{12}, \omega_1, \omega_2)$ and $u^{\mu Q}(r_{12}, \omega_1, \omega_2)$ are the quadrupole–quadrupole and dipole–quadrupole potentials, respectively. The Kihara potential [50] is given by

$$u^K(r_{12}, \omega_1, \omega_2) = 4\epsilon \left[\left(\frac{\sigma}{\rho} \right)^{12} - \left(\frac{\sigma}{\rho} \right)^6 \right]. \quad (2.2)$$

In this equation, ϵ and σ are the energy depth and size parameters, respectively. The dipole–dipole potential [51] is given by,

$$u^{\mu\mu}(r_{12}, \omega_1, \omega_2) = \frac{\mu^2}{r_{12}^3} (c\gamma_{12} - 3c_1c_2), \quad (2.3)$$

and the quadrupole–quadrupole potential is,

$$u^{QQ}(r_{12}, \omega_1, \omega_2) = \frac{3Q^2}{4r_{12}^5} \left[1 - 5(c_1^2 + c_2^2 + 3c_1^2c_2^2) + 2(c\gamma_{12} - 5c_1c_2)^2 \right]. \quad (2.4)$$

Finally the dipole–quadrupole potential is,

$$u^{\mu Q}(r_{12}, \omega_1, \omega_2) = \frac{3\mu Q}{2r_{12}^4} c_{12} [1 + 5c_1c_2 - 2c\gamma_{12}] \quad (2.5)$$

where $\rho(r_{12}, \omega_1, \omega_2)$ is the shortest distance between the molecular cores, $c_i = \cos\theta_i$, $s_i = \sin\theta_i$, $c_{ij} = \cos(\theta_i - \theta_j)$ and $c\gamma_{ij} = \cos\theta_i \cos\theta_j + \sin\theta_i \sin\theta_j \cos(\phi_i - \phi_j)$.

2.2. Simulation method

The vapor–liquid coexistence of multipolar Kihara spherocylinders was determined with the Gibbs ensemble Monte Carlo (GEMC) simulation technique [52]. This method is frequently used to determine the vapor–liquid phase equilibrium (VLE) of spherical pure fluids and extended to mixtures [15,52–55]. We have obtained the VLE of multipolar linear Kihara fluids of unitless length $L^* = L/\sigma = 0.3, 0.6$, and 0.8 using the Gibbs ensemble technique. GEMC simulations of 512 particles were performed. The particles were uniformly distributed in two boxes of equal volumes and number of particles at a unitless temperature T^* . The Monte Carlo sequence was performed by sampling configurations with displacements of particles, interchange of particles between the two boxes, and volume exchange trials. The potential energy required for the MC sampling, and the minimum distance between molecular pairs of cores are evaluated by a modification of the Vega and Lago algorithm [56]. The average of the observables were obtained as statistical averages after a production run of 3×10^6 MC cycles preceded by an equilibration stage of 1.5×10^6 MC cycles. For instance, the configurational pressure was evaluated using the virial theorem as $p_{vir} = -\rho/2 \langle \sum_{i<j} \mathbf{r}_{ij} \mathbf{v}_{ij} (\partial u_K(\rho_{ij}) / \partial \rho_{ij}) \rangle$, where $\langle \cdot \rangle$ stands for ensemble average and \mathbf{v}_{ij} is the unit vector in the direction of ρ_{ij} . The potential was truncated at a cutoff distance of $\rho_c = 3\sigma$ and long-tail corrections were added. In the case of polar fluids, two main methods have been developed to deal with long-range interactions: (i) the Ewald summations method [57] and (ii) the reaction field (RF) approach [58]. In this work, we used the RF approach to account the long-range dipolar interactions with the RF dielectric constant set equal in both phases ($\epsilon_{RF}(\text{liquid}) = \epsilon_{RF}(\text{vapor}) = \infty$). It has been previously demonstrated that simulations using the Ewald summations method yield identical results to RF technique [59].

Each MC cycle comprised one displacement trial per particle and one attempt to change the total volume and another attempt of interchanging a particle between the boxes. The acceptance *ratio* of particles displacements and area exchange were around 40%. Error bars are estimated from the standard deviations of the average values of the thermodynamic variables obtained over 100 MC cycles.

Our code has been tested against database correlations [60] and also against the compressibility factor test [61,62]. The results are presented in the Supporting Information for those readers interested in this benchmark model. As a general comment, the simulation results of the Lennard-Jones model passed the test. The average absolute deviations (AAD) of our results against the correlation presented in Ref. [60] is $\sim 0.2\%$. However, in the point which is closer to the critical temperature, the compressibility factor tested lead to deviations higher than 1.2%. This point was used as an advice note for not simulating thermodynamics states in the vicinity of the critical region. However, the critical temperature and density deviates less than 1% with respect to the benchmark data in Ref. [60].

To estimate the critical temperature (T_c^*) and critical density (ρ_c^*), we used the scaling law and the rectilinear diameters recipe as a first estimate for the Wegner expansion [63]. The simulation data were fitted to the following expression,

$$\rho_{\pm}^* = \rho_c^* + B_0|t| \pm \frac{1}{2}B_1|t|^\alpha, \quad (2.6)$$

where ρ_+^* and ρ_-^* stand for the vapor and liquid densities, respectively, and $t = 1 - T^*/T_c^*$. The fitting parameters α and the amplitude terms B_0 and B_1 are also obtained in the procedure and incorporated in the Supporting Information. As expected, the critical exponent α remains close to 1/3 within the estimated uncertainties. The amplitude term B_1 , that provides information about the width of the diagram, increases with the multipole moment as expected.

The critical pressure, p_c^* , was obtained by fitting the vapor–pressure data to the Antoine equation,

$$\ln p_c^* = A + \frac{B}{T_c^*}, \quad (2.7)$$

where A and B are fitting parameters. The critical pressure, p_c^* , was obtained at the corresponding value of T_c^* obtained from Eq. (2.6). The collection of simulation data are reported in tabular form in the Supporting Information.

2.3. Perturbation theory (PT)

In the generalized framework provided by the discrete perturbation theory (DPT), the authors have successfully developed subsequent extensions to molecular fluids of different shapes in two- and three-dimensions, including multipolar interactions. Here, we incorporate the multipolar interaction in cases where both dipole and quadrupole moments are presented. Briefly, in the DPT for molecular fluids (mol-DPT), the Helmholtz free energy $a = A/NkT$ of a system comprised by N molecules contained within a volume V at temperature T , and with unitless density $\rho^* = (N/V)\sigma^3$ can be written as,

$$a = \Psi_0 + \ln \rho^* + a_0 + a_{exc}, \quad (2.8)$$

where σ a characteristic length of the reference potential (i.e. the diameter in the case of the hard-sphere (HS) model), k the Boltzmann constant and (Ψ_0) the temperature-dependent contribution of the internal degrees of freedom of the ideal gas. The a_0 stands for the contribution of the selected reference potential. Here, we used the HS free energy term through the Carnahan–Starling equation of state [64]. Finally, there are three contributions to the excess free energy (a_{exc}): the perturbation part of the Kihara potential (a^{att}), the multipolar terms (a^M) and a crossed Kihara-multipolar term. The latter term is of third order in inverse temperature and consequently can be safely neglected. It should be remarked that the theory is constructed by spherulized SW steps and hence no crossed Kihara-multipolar terms appears in

the expansion. This approach simplifies the problem that arises when considering anisotropic excluded volume interactions as it is the case of the Kihara model.

The treatment of the first term is considered with the Barker–Henderson based DPT [65–67] that generates analytical equations of state (EOSs) in the parameters that characterize the intermolecular interactions. Explicitly, the unitless excess Helmholtz free-energy a^{att} for a perturbative potential is mapped into a SW-sequence like n steps of range λ_i . The extraction of an analytical expression for the discrete excess Helmholtz free energy at second order in β were performed by Benavides and Gil-Villegas [65] by noticing that first and second order SW perturbation terms are related to those of a square-shoulder (SS) in a very simple way: $a_1^{SS}(\rho^*, \lambda) = -a_1^{SW}(\rho^*, \lambda)$ and $a_2^{SS}(\rho^*, \lambda) = a_2^{SW}(\rho^*, \lambda)$, making possible the study of several atomic models with only the knowledge of suitable expressions for those perturbation corrections to the ideal Helmholtz free energy of a SW fluid of variable range λ : $a_1(\rho^*, \lambda)$ and $a_2(\rho^*, \lambda)$ in which the original potential is mapped. Hence:

$$\begin{aligned} a^{att}(\rho^*, \lambda_i, \epsilon_i, \beta) = & \beta \sum_i^n [a_1^S(\rho^*, \lambda_i, \epsilon_i) - \left(\frac{\epsilon_i}{\epsilon_{i-1}}\right) a_1^S(\rho^*, \lambda_{i-1}, \epsilon_i)] + \\ & \beta^2 \sum_i^n [a_2^S(\rho^*, \lambda_i, \epsilon_i) - \left(\frac{\epsilon_i}{\epsilon_{i-1}}\right)^2 a_2^S(\rho^*, \lambda_{i-1}, \epsilon_i)] \end{aligned} \quad (2.9)$$

where $\beta = 1/kT$, the terms a_1^S and a_2^S are the first- and second-order Helmholtz free energy perturbation terms of either a SW or SS fluid depending on the sign of ϵ_i , the corresponding minimum energy parameter of the interaction. Here, in both the treatment of the reference model and excess contributions for non-spherical particles, one has to define the effective range λ_{eff} of the i th step of the attractive part by considering that the volume of the attractive shell of the attractive spherical SW' with thickness $\sigma^{eff}(\lambda_i^{eff} - 1)$ and the equivalent volume of the non-spherical SW defining each step of the discrete potential are equal. Specific results for σ^{eff} and λ_i^{eff} for different molecular geometries can be found in Ref. [47]. The contributions of each SW steps will be evaluated applying the EOS of Espíndola et al. [68] for ranges $1.2 \leq \lambda \leq 3$, and Benavides and del Río [69] expressions for longer SW ranges.

The contribution arising from the electrostatic interactions a^M is incorporated with the Padé approximate expression valid for low and moderate values of unitless multipole moments-for multipolar HS developed by Larsen et al. [70] that gives an accurate estimation of the polar series in terms of the second (a_2^M) and third (a_3^M) perturbation terms as follows [71]

$$a^M = \frac{a_2^M}{T^{*2}} \left(1 - \frac{a_3^M}{T^* a_2^M} \right)^{-1}. \quad (2.10)$$

Incidentally, this exactness falls into the multipolar range of real substances [72]. In this expression, the terms a_2^M and a_3^M are written as polynomials in ρ^* whose coefficients can be found in Ref. [73]. Moreover, unitless multipole moments and multipole densities will be defined. The unitless dipole, μ^{*2} , is defined as,

$$\mu^{*2} = \frac{\mu^2}{\epsilon \sigma^3}, \quad (2.11)$$

the unitless quadrupole moment,

$$Q^{*2} = \frac{Q^2}{\epsilon \sigma^5}, \quad (2.12)$$

and finally,

$$\mathcal{M}^{*2} = \frac{\mu^2}{\epsilon V_m} + \frac{Q^2}{\epsilon V_m^{5/3}}, \quad (2.13)$$

where \mathcal{M}^{*2} is the unitless multipole density. This definition is consistent with those reported in Refs. [11,12,24,27] for dipole and quadrupole densities.

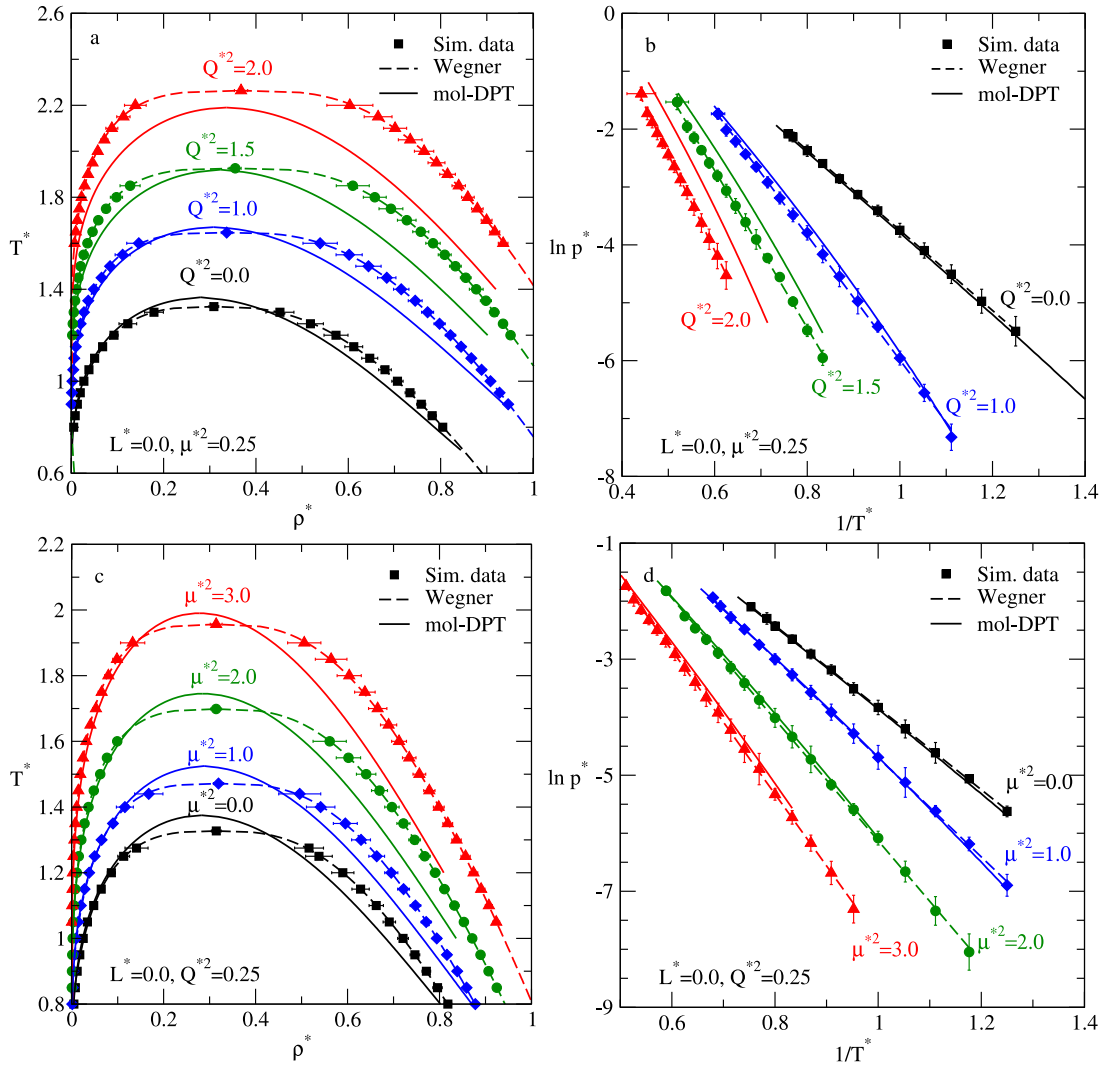


Fig. 1. Panel (a): Density–temperature projection of the vapor–liquid coexistence envelope for Lennard-Jones fluids with a dipolar moment of $\mu^{*2} = 0.25$ and different values of Q^{*2} . Panel (b): The same as in panel (a) but in the vapor pressure–temperature projection. Panel (c): Density–temperature projection of the vapor–liquid coexistence envelope for Lennard-Jones fluids with quadrupolar moment $Q^{*2} = 0.25$ and different values of μ^{*2} . Panel (d): The same as in panel (c) but in the vapor pressure–temperature projection. The filled symbols are the GEMC results, the dashed lines correspond to the Wegner expansion and the solid lines stand for the results obtained from the mol-DPT approach.

Details about the implementation of the free energy for the Kihara contribution are provided in Ref. [47]. For the evaluation of the multipolar contribution, a word of caution is relevant. The unitless molecular value of the multipole M^* should be incorporated in an effective way, i.e.,

$$M_{eff}^{*2} = \frac{M^{*2}}{\epsilon \sigma_{eff}^{(2l+1)/3}}, \quad (2.14)$$

where $l = 1$ or 2 for dipole or quadrupole moments, respectively. For a prolate spherocylinder the value of $\sigma_{eff}^3 = 1 + 1.5L^*$. Overall, dimensionless form, the theory has four free parameters: (1) the number of steps in which the Kihara potential is splitted according to the standard DPT prescriptions, (2) the molecular elongation (L^*), (3) the dipole moment (μ^*), and (4) the quadrupole moment Q^* .

The so-obtained free energy can be compared directly against simulation results for the equation of state. However, the determination of liquid–vapor phase boundaries that arises from the conditions of thermal, mechanical and chemical equilibrium constitutes a more severe test not only for an equation of state, but for their first derivatives respect to volume (i.e., the pressure, p) and number of particles (the chemical potential). The FORTRAN code in which the calculation of the free energy is implemented is available from the authors upon

reasonable request. The perturbation theory has been also tested for the Lennard-Jones case against the benchmark database set in Ref. [60] as presented in [74] for temperatures below $0.8T_c^* \approx 1.06$. Despite the mol-DPT is not empirically, parametrized, the AAD of 150 data of equilibrium vapor and liquid densities is 6%, which is of the same order of magnitude that the ADD of some of the Lennard-Jones EOSs collected in Ref. [74], some of them with fitted coefficients that account for particular simulation data.

3. Results

We have calculated the VLE data for a set of 64 fluid models covering unitless lengths in the interval $L^* \in [0, 0.8]$ by means of GEMC. For each length, two different subset of models were considered. First, we fixed $\mu^{*2} = 0.25$ and Q^{*2} were varied between 0 and 2. Identically, the VLE of a second set of models were evaluated by fixing $Q^{*2} = 0.25$ while μ^{*2} ranges between 0 and 3.

In Figs. 1–2 we present both the GEMC simulation results and the mol-DPT predictions of the VLE results for a selected set of Kihara models with different values of L^* , μ^* and Q^* . Particularly, in Fig. 1(a) and (b), the VLE and vapor–pressure curves obtained by the mol-DPT approach and GEMC simulations for dipolar Kihara fluids ($\mu^{*2} = 0.25$)

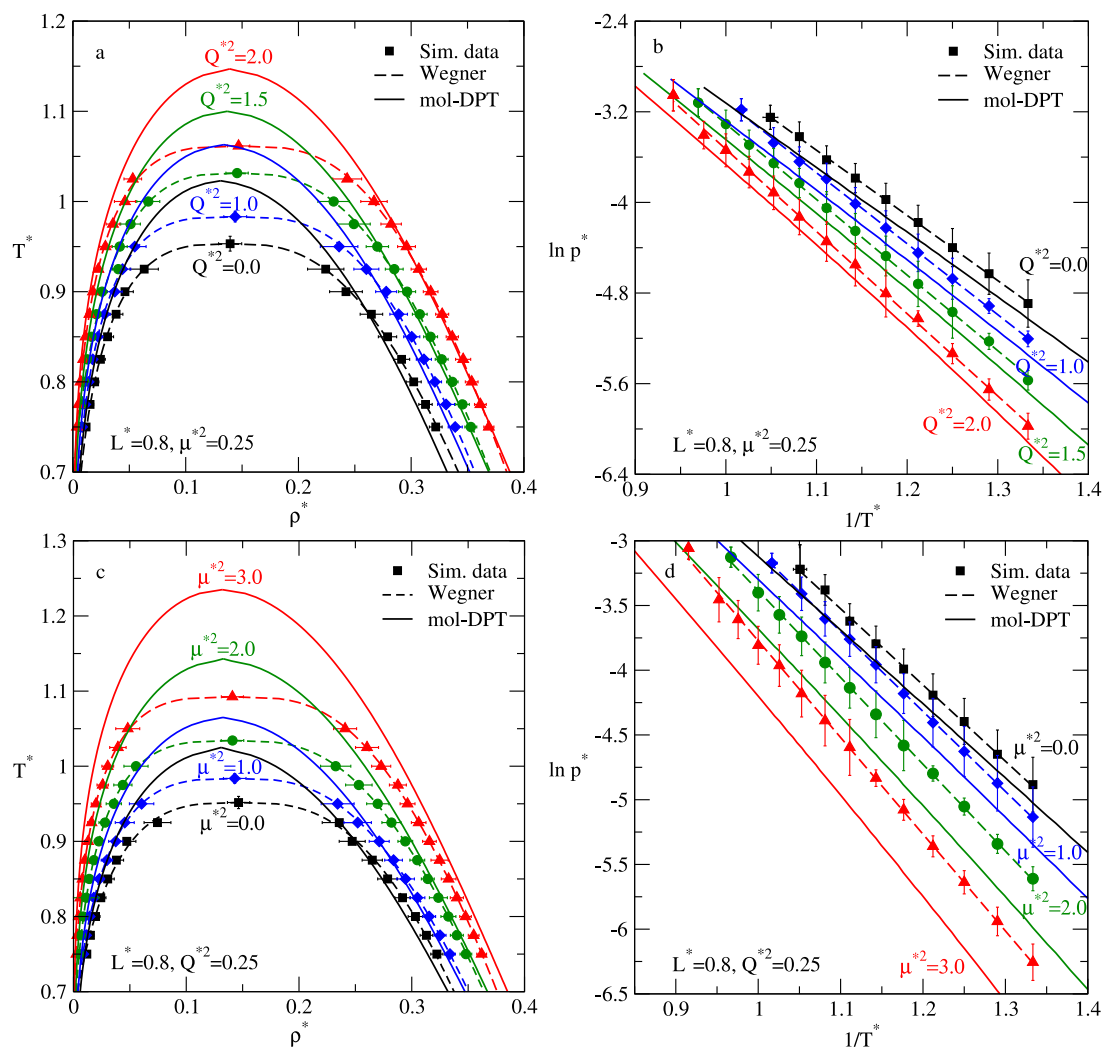


Fig. 2. Panel (a): The same as in Fig. 1a but for Kihara fluids of $L^* = 0.80$. Panel (b): The same as in panel (a) but in the vapor pressure–temperature projection. Panel (c): The same as in Fig. 1c but for Kihara fluids of $L^* = 0.80$. Panel (d): The same as in panel (c) but in the vapor pressure–temperature projection.

for several values of the unitless squared quadrupole moment Q^{*2} (0.0, 1.0, 1.5, and 2.0) are shown. Similarly, the VLE coexistence and vapor-pressure for dipolar Kihara fluids ($L^* = 0.80$, and $\mu^{*2} = 0.25$) for several values of the quadrupole moment $Q^{*2} = 0.0, 1.0, 1.5$, and 2.0 are shown in Fig. 2(a) – (b). The complete set of data are presented in the Supporting Information. Additionally, the performance of the mol-DPT approach is compared with GEMC results. Simulations results are plotted as full symbols and VLE calculated with mol-DPT as continuous lines. Wegner expansion fits to GEMC data are also included as dashed lines. As a whole we found that the mol-DPT theory just outlined gives semiquantitative result for this wide set of anisotropic molecular models of Kihara features.

Briefly, for a given elongation, GEMC and mol-DPT show an increment in the critical temperature and, consequently, a widening of the coexistence curves as the multipole moment increases, either dipole and/or quadrupole moment. This feature has been previously observed in dipolar and quadrupolar models. As discussed in Refs. [11,24,59] the quadrupole and dipole moments decreases the vapor-pressure at a given temperature. As it is well known the slope of the Clausius-Clapeyron projections ($\ln p^*$ versus $1/T^*$) showed in right panels of Figs. 1–2 are related with the vaporization enthalpy. It becomes apparent that the vaporization enthalpy increases with the multipole moment, especially at low temperatures.

Overall, the effects of the multipole moment becomes more significant as the molecular length diminishes since the elongation narrow the

VLE boundaries [10]. In other words, as the molecular shape becomes more isotropic the effect of the multipoles is much more significant. In general terms, we observed a good agreement between mol-DPT and GEMC the simulation data. However, as Q^{*2} becomes larger the theoretical predictions are only in qualitative agreement, particularly close to the critical point. The deterioration of the theoretical predictions rests in: (i) the fact the Padé approximant functionality employed to reproduced the multipolar expansion stops fulfilling at large values of the multipole moment because of non-convergence of the series; (ii) the presence of a quadrupole moment has a strongest impact in the VLE when plotted in a unitless scale. Hence, despite critical properties are only qualitatively predicted by the mol-DPT (as expected from a perturbation theory), the predictions of the orthobaric densities and vapor pressures are semiquantitative for temperatures below $\sim 0.8T_c^*$. Although there exist some classical works dealing with perturbation theories in the literature [38,39], only the equation of state are compared with experimental or simulations results. However it is well known that the agreement in this properties does not guarantee an agreement in the equilibrium boundaries, and the mol-DPT is, to the best of our knowledge, the first perturbation theory tested against simulation data with a degree of agreement similar to those found for multipolar atomic fluids [13,14,17].

For that reason, the absolute values of the critical properties coming from GEMC and mol-DPT are difficult to be compared directly. Hence, in Fig. 3 we presented the collected results for critical properties

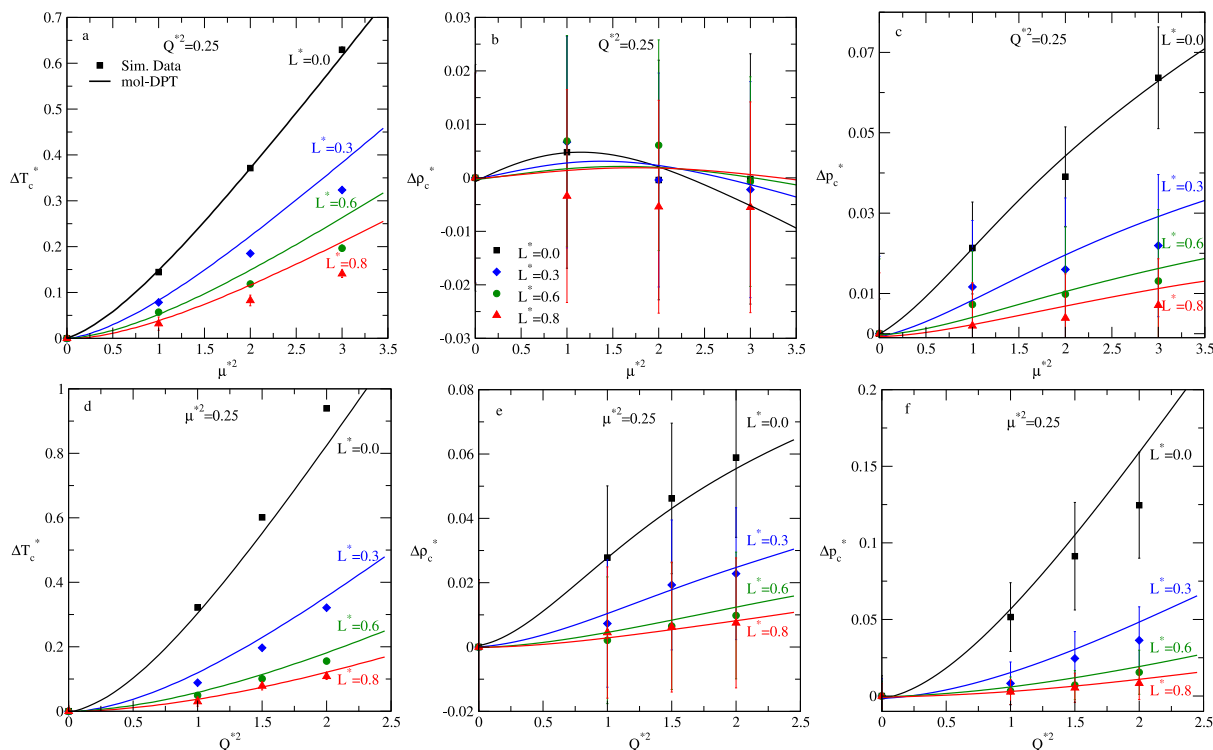


Fig. 3. Panel (a): Critical temperature as function of the unitless dipole for Kihara fluids with $Q^{*2} = 0.25$. Panel (b)–(c): the same as in panel (a) but for critical density and pressure, respectively. Panel (d): Critical temperature as function of the unitless quadrupole for Kihara fluids with $\mu^{*2} = 0.25$. Panel (e)–(f): the same as in panel (d) but for critical density and pressure, respectively. The filled symbols are the GEMC results and the solid lines correspond to the mol-DPT approach.

for all the systems treated by plotting the relative critical properties (i.e. the critical property of a given model with respect to the nonpolar spherocylinder of the same length) against the unitless dipole (for systems with variable Q^*) or quadrupole (for systems with variable μ^*). Although anisotropic models are known not to follow the principle of corresponding states, these curves allow us to find molecular models whose critical behavior might be similar to another with different length and multipole moment. For instance, from Fig. 2 it is clear than a Kihara spherocylinder with $L^* = 0.8$, $Q^{*2} = 0.25$ and $\mu^{*2} = 3$ would show a similar critical properties to that with $L^* = 0$, $Q^{*2} = 0.25$ and $\mu^{*2} \sim 0.75$. A close inspection to this (or close to) models among the reported results reflects that, despite critical properties are similar in those models, the liquid densities at equilibrium are different by a factor of about 2. This fact indicates that molecular anisotropy and multipole moment affects in a very different extension to the non-conformal behavior of the model and modulates molecular properties in non-identical directions. Particularly, the increment in the critical temperature demonstrated that this property is dominated by electrostatic effects, while orthobaric densities are mainly controlled by molecular anisotropy. Finally, it ought to be mentioned that the opposite effect of elongations and multipole moment in the critical temperature and coexistence densities lead to a paradoxical situation: as commented previously, while it is well established that elongation and multipole cause deviations from the CSP [10–12], when both anisotropy source (geometrical and charge density asymmetries) these effects on the CSP are cancelled out. This point is presented in Figure S3 of the Supporting Information, where a representation of the reduced densities, $\rho_R = \rho^*/\rho_c^*$ as a function of the reduced temperature $T_R = T^*/T_c^*$ is presented for a dipolar model with $\mu^{*2} = 0.25$ and a varying quadrupole moment for the Lennard-Jones and the $L^* = 0.8$ Kihara spherocylinder. Deviations from the CSP are apparent in the $L^* = 0$ model whilst curves overlaps in the elongated model.

Besides, in all cases, both dipole and quadrupole does not affect strongly the critical density at moderate multipole values. However, at higher values of the dipole moment, the mol-DPT predicts a slight

decrease in the critical densities in comparison with the corresponding nonpolar model. Because of the uncertainties in the simulation results as derived from the Wegner expansion, it is hard to say whether this trend is real or its an artifact of the low temperature expansion employed in the mol-DPT. Nonetheless, this trend was previously reported for polar Kihara and Stockmayer fluids [15] and can be considered reliable, since it has been reported to be a consequence of a polymerization effects of the dipolar particles [75].

Nevertheless, and as shown previously (Refs. [11,12] and references therein), defining a length-dependent reduce multipole moment constitute a route to provide a comprehensive effect of the multipole/length balance on the vapor–liquid equilibria. As mentioned in the Methods section, we defined the unitless multipole density \mathcal{M} to incorporate excluded volume effects on the molecular electrostatic features. This simple operation favors that the comparison between theoretical and simulation results and we found a universal curve for the critical properties of the simulated models against \mathcal{M}^2 as presented in Fig. 4. We observed a monotonous increment of the critical temperature with \mathcal{M}^2 , while critical densities started to diminish at $\mathcal{M}^2 \gtrsim 3$. These effects are more pronounced than in purely polar and quadrupolar models, because of the synergic effect of dipoles and quadrupoles, that leads to an additional source of free energy minimization [26]. The more surprising feature of these curves is that critical saturation pressures are almost constant in the \mathcal{M} range considered here, provided vapor pressures change several orders of magnitude with the temperature.

4. Conclusions

The molecular discrete perturbation theory has been tested against GEMC simulation results for dipolar and quadrupolar Kihara spherocylinders. The theoretical predictions are in remarkably good agreement with Monte Carlo simulations. These results constitute a complete and systematic theoretical and computational picture of the effect of the balanced effect of the anisotropies coming from either the spherocylinder elongation and the multipole expansion on the thermodynamic of

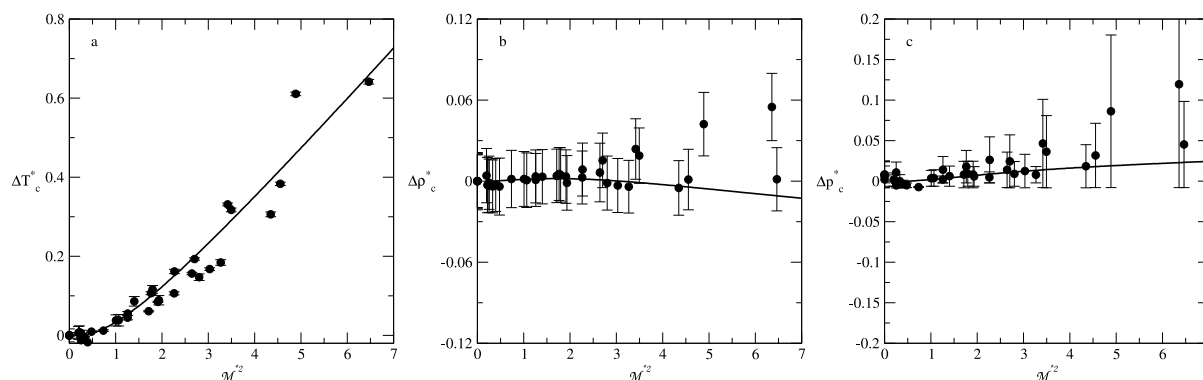


Fig. 4. Panel (a): Unitless critical temperature as function of the unitless density of multipole, M^2 for Kihara fluids. Panel (b)–(c): the same as in panel (a) but for the unitless critical density and pressure, respectively. The filled symbols are the GEMC results, and the solid lines correspond to the mol-DPT approach, respectively.

molecular fluids with prolate geometry. We found similar but marked trends as those observed in the literature for dipolar and quadrupolar models.

Although theoretical predictions can be considered reliable and adequate for practical purposes, the incorporation of terms of order higher-than-two into the mol-DPT would benefit our proposal towards an analytical, accurate and versatile equations of state that also provides good description of the characteristic asymptotic behavior in the critical region [76,77].

In summary, the results of the present work validate the predictions of the theoretical equation of state except for the absolute values of the critical properties and convert it into a useful and easily extendable tool to explore, for instance, the adsorption of mixtures of molecular fluids or concentration dependent features of asymmetric colloidal suspensions. Finally, our results can be extended to the calculation of thermodynamic properties of mixtures of molecular fluids with multipole moments. Research in these directions are currently underway in our group.

CRedit authorship contribution statement

Víctor M. Trejos: Methodology, Software, Data curation, Writing – review & editing. **Francisco Gámez:** Methodology, Software, Writing – original draft, Writing – review & editing.

Declaration of competing interest

The authors declare that they have no known competing financial interests or personal relationships that could have appeared to influence the work reported in this paper.

Data availability

Data will be made available on request.

Acknowledgments

V.M.T. acknowledges the Mexican Ministry of Education (SEP) for the financial support (projects UAEH-PTC-831 and “Apoyo a Profesores con Perfil Deseable”). F.G. also thanks funding through the Ministerio de Ciencia e Innovación de España, Spain (PID2019-105195RA-I00). We really appreciate the comments and suggestions of Dr. Benito Garzón and Ariadna Selene Garcilazo that certainly enriched the discussion of the results.

Appendix A. Supplementary data

Supplementary material related to this article can be found online at <https://doi.org/10.1016/j.cplett.2022.140171>.

References

- [1] B.J. Berne, P. Pechukas, Gaussian model potentials for molecular interactions, *J. Chem. Phys.* 56 (1972) 4213–4216.
- [2] J.G. Gay, B.J. Berne, Modification of the overlap potential to mimic a linear site-site potential, *J. Chem. Phys.* 74 (1981) 3316–3319.
- [3] T. Kihara, The second virial coefficient of Non-Spherical molecules, *J. Phys. Soc. Japan* 6 (1951) 289–296.
- [4] T. Kihara, *Adv. Chem. Phys.* 33 (1975) 51.
- [5] T. Kihara, Intermolecular core-potential depth versus critical temperature, *Chem. Phys. Lett.* 92 (1982) 175–177.
- [6] M. Bohn, R. Lustig, J. Fischer, Description of polyatomic real substances by two-center Lennard-Jones model fluids, *Fluid Phase Equilib.* 25 (1986) 251–262.
- [7] M. Bohn, B. Saager, K. Holzapfel, J. Fischer, Studies on phase equilibria of two-centre Lennard-Jones fluids, *Mol. Phys.* 59 (1986) 433–440.
- [8] C. Kriebel, A. Müller, J. Winkelmann, Vapour-liquid equilibria of two-centre Lennard-Jones fluids from the NpT plus test particle method, *Mol. Phys.* 84 (1995) 381–394.
- [9] A. Friedrich, R. Lustig, Thermodynamic properties of model molecules with hexagonal symmetry from statistical mechanical theory, *J. Chem. Phys.* 105 (1996) 9597–9614.
- [10] C. Vega, S. Lago, E. de Miguel, L.F. Rull, Liquid-vapor equilibria of linear Kihara molecules, *J. Phys. Chem.* 96 (1992) 7431–7437.
- [11] B. Garzón, S. Lago, C. Vega, L.F. Rull, Computer simulation of vapor-liquid equilibria of linear dipolar fluids: Departures from the principle of corresponding states, *J. Chem. Phys.* 102 (1995) 7204–7215.
- [12] B. Garzón, S. Lago, C. Vega, L.F. Rull, Computer simulation of vapor-liquid equilibria of linear quadrupolar fluids: Departures from the principle of corresponding states, *J. Chem. Phys.* 101 (1994) 4166–4176.
- [13] A.L. Benavides, S. Lago, B. Garzón, L.F. Rull, F.D. Río, Liquid-vapour equilibrium of multipolar square-well fluids. Gibbs ensemble simulations and equation of state, *Mol. Phys.* 103 (24) (2005) 3243–3251.
- [14] M.E.V. Leeuwen, B. Smit, E.M. Hendriks, Vapour-liquid equilibria of Stockmayer fluids Computer simulations and perturbation theory, *Mol. Phys.* 78 (1993) 271–283.
- [15] B. Smit, C. Williams, E. Hendriks, S.D. Leeuw, Vapour-liquid equilibria for Stockmayer fluids, *Mol. Phys.* 68 (1989) 765–769.
- [16] M.V. Leeuwen, Deviation from corresponding-states behaviour for polar fluids, *Mol. Phys.* 82 (1994) 383–392.
- [17] F. Alavi, F. Feyzi, An equation of state contribution for dipolar and quadrupolar square-well fluids, *Mol. Phys.* 106 (2008) 161–174.
- [18] A. Benavides, F. Gámez, Perturbation theory for multipolar discrete fluids, *J. Chem. Phys.* 135 (2011) 134511(1)–134511(8).
- [19] A.L. Benavides, F.J.G. Delgado, F. Gámez, S. Lago, B. Garzón, Statistical thermodynamics of fluids with both dipole and quadrupole moments, *J. Chem. Phys.* 134 (2011) 234507.
- [20] I.I. Alkhatib, L.M.C. Pereira, J. Torne, L.F. Vega, Polar soft-SAFT: Theory and comparison with molecular simulations and experimental data of pure polar fluids, *Phys. Chem. Chem. Phys.* 22 (2020) 13171–13191.
- [21] H. Zhao, P. Morgado, A. Gil-Vilegas, C. McCabe, Predicting the phase behavior of nitrogen + *n*-alkanes for enhanced oil recovery from the SAFT-VR approach: Examining the effect of the quadrupole moment, *J. Phys. Chem. B* 110 (2006) 24083–24092.
- [22] H. Zhao, Y. Ding, C. McCabe, Phase behavior of dipolar associating fluids from the SAFT-VR+D equation of state, *J. Chem. Phys.* 127 (2007) 084514(1)–084514(12).
- [23] A. Benavides, Y. Guevara, F. del Río, Vapor-liquid equilibrium of a multipolar square-well fluid: I. Effect of multipolar strengths, *Physica A* 202 (1994) 420–437.

- [24] B. Garzón, S. Lago, C. Vega, Monte Carlo simulations of dipolar and quadrupolar linear kihara fluids. A test of thermodynamic perturbation theory, *Mol. Phys.* 96 (1999) 123–132.
- [25] J. Vrabec, J. Gross, Vapor-liquid equilibria simulation and an equation of state contribution for dipole-quadrupole interactions, *J. Phys. Chem. B* 112 (2008) 51–60.
- [26] G.S. Dubey, S.F. O'Shea, Phase equilibria of Lennard-Jones dipolar plus quadrupolar fluids by Gibbs-ensemble Monte Carlo simulation, *Phys. Rev. E* 49 (1994) 2175–2183.
- [27] S. Lago, B. Garzón, S. Calero, C. Vega, Accurate simulations of the vapor-liquid equilibrium of important organic solvents and other diatomics, *J. Phys. Chem. B* 101 (1997) 6763–6771.
- [28] K.E. Gubbins, N. Quirke, *Molecular Simulation and Industrial Applications: Methods, Examples and Prospects*, Gordon and Breach, Amsterdam, 1996.
- [29] S. Stephan, M.T. Horsch, J. Vrabec, H. Hasse, MolMod - an open access database of force fields for molecular simulations of fluids, *Mol. Simul.* 45 (2019) 806–814.
- [30] C. Kriebel, M. Mecke, J. Winkelmann, J. Vrabec, J. Fischer, An equation of state for dipolar two-center Lennard-Jones molecules and its application to refrigerants, *Fluid Phase Equilib.* 142 (1998) 15–32.
- [31] J. Stoll, J. Vrabec, H. Hasse, J. Fischer, Comprehensive study of the vapour-liquid equilibria of the pure two-centre Lennard-Jones plus pointquadrupole fluid, *Fluid Phase Equilib.* 179 (2001) 339–362.
- [32] J. Stoll, J. Vrabec, H. Hasse, Comprehensive study of the vapour-liquid equilibria of the pure two-centre Lennard-Jones plus pointdipole fluid, *Fluid Phase Equilib.* 209 (2003) 29–53.
- [33] S. Calero, A new and more direct test of Hubbard relations from molecular mass distribution influence on linear liquid dynamics, *J. Chem. Phys.* 111 (1999) 5434–5440.
- [34] C. Vega, S. Lago, Perturbation theory of angular molecules interacting through the Kihara potential, *J. Chem. Phys.* 94 (1991) 310–320.
- [35] C. Vega, S. Lago, P. Padilla, Thermodynamic properties of nonpolar molecular fluids of different geometries from perturbation theory, *J. Phys. Chem.* 96 (1992) 1900–19005.
- [36] S. Calero, B. Garzón, S. Lago, Influence of charge distribution on the thermophysical and dynamical properties of polar linear molecules, *J. Chem. Phys.* 118 (2003) 11079–11091.
- [37] S. Calero, B. Garzón, L.G. MacDowell, S. Lago, Nonequilibrium properties of linear polar kihara fluids from molecular dynamics. Results for models and for liquid acetonitrile, *J. Chem. Phys.* 107 (1997) 2034–2045.
- [38] T. Boublík, Equilibrium behaviour of quadrupolar Kihara molecule fluids, *Mol. Phys.* 73 (1991) 417–426.
- [39] T. Boublík, Perturbation theory of polar nonspherical molecule fluids, *Mol. Phys.* 76 (1992) 327–336.
- [40] C. Vega, B. Garzón, L.G. MacDowell, S. Lago, Vapour-liquid equilibria of propane and *n*-alkane conformers, *Mol. Phys.* 85 (1995) 679–699.
- [41] A.L. Benavides, L.A. Cervantes, J. Torres, Discrete perturbation theory for the Jagla Ramp potential, *J. Phys. Chem. C* 111 (2007) 16006–16012.
- [42] N.E. Valadez-Pérez, A.L. Benavides, E. Schöell-Passinger, R. Castañeda-Priego, Phase behavior of colloids and proteins in aqueous suspensions: Theory and computer simulations, *J. Chem. Phys.* 137 (2012) 084905(1)–084905(15).
- [43] J. Cui, J.R. Elliott Jr., Phase diagrams for a multistep potential model of *n*-alkanes by discontinuous molecular dynamics and thermodynamic perturbation theory, *J. Chem. Phys.* 116 (2002) 8625–8631.
- [44] G.A. Chapela, L.E. Scriven, H.T. David, Molecular dynamics for discontinuous potential. IV. Lennard-Jonesium, *J. Chem. Phys.* 91 (1989) 4307–4313.
- [45] J.R. Elliott, N.H. Gray, Asymptotic trends in thermodynamic perturbation theory, *J. Chem. Phys.* 123 (2005) 184902(1)–184902(6).
- [46] V.M. Trejos, A. Santos, F. Gámez, Vapor-liquid equilibrium and equation of state of two-dimensional fluids from a discrete perturbation theory, *J. Chem. Phys.* 148 (2018) 194505.
- [47] F. Gámez, A.L. Benavides, Perturbation theory for non-spherical fluids based on discretization of the interactions, *J. Chem. Phys.* 138 (2013) 124901(1)–124901(7).
- [48] F. Gámez, Thermodynamic of fluids from a general equation of state: The molecular discrete perturbation theory, *J. Chem. Phys.* 140 (2014) 234504(1)–234504(4).
- [49] F. Gámez, L.F. R.-Almeida, V.M. Trejos, Thermodynamics of two-dimensional molecular fluids: Discrete perturbation theory and Monte Carlo simulations, *J. Mol. Liq.* 300 (2020) 112293(1)–112293(9).
- [50] T. Kihara, Virial coefficients and models of molecules in gases, *Rev. Modern Phys.* 25 (1953) 831–843.
- [51] W.H. Stockmayer, Second virial coefficients of polar gases, *J. Chem. Phys.* 9 (1941) 398–402.
- [52] A.Z. Panagiotopoulos, Direct determination of phase coexistence properties of fluids by Monte Carlo simulation in a new ensemble, *Mol. Phys.* 61 (1987) 813–826.
- [53] A.Z. Panagiotopoulos, N. Quirke, M. Stapleton, D.J. Tildesley, Phase equilibria by simulation in the Gibbs ensemble Alternative derivation, generalization and application to mixture and membrane equilibria, *Mol. Phys.* 63 (1988) 527–545.
- [54] E.N. Rudsill, P.T. Cummings, Gibbs ensemble simulation of phase equilibrium in the hard core two-Yukawa fluid model for the Lennard-Jones fluid, *Mol. Phys.* 68 (1989) 629–635.
- [55] V.I. Harisimadis, N.K. Koutras, D.P. Tassios, A.Z. Panagiotopoulos, How good is conformal solutions theory for phase equilibrium predictions? *Fluid Phase Equilib.* 65 (1991) 1–18.
- [56] C. Vega, S. Lago, A fast algorithm to evaluate the shortest distance between rods, *Comput. Chem.* 18 (1994) 55–59.
- [57] S.W. de Leeuw, J.W. Perram, E.R. Smith, Simulation of electrostatic systems in periodic boundary conditions. II. Equivalence of boundary conditions, *Proc. R. Soc. Lond. Ser. A Math. Phys. Eng. Sci.* 373 (1980) 57–66.
- [58] J.A. Barker, R.O. Watts, Monte Carlo studies of the dielectric properties of water-like models, *Mol. Phys.* 26 (1973) 789–792.
- [59] B. Garzón, S. Lago, C. Vega, Reaction field simulations of the vapor-liquid equilibria of dipolar fluids. Does the reaction field dielectric constant affect the coexistence properties? *Chem. Phys. Lett.* 231 (1994) 366–372.
- [60] S. Stephan, M. Thol, J. Vrabec, H. Hasse, Thermophysical properties of the lennard-jones fluid: Database and data assessment, *J. Chem. Inf. Model.* 59 (2019) 4248–4265.
- [61] I. Nezbeda, Simulations of vapor-liquid equilibria: Routine versus thoroughness, *J. Chem. Eng.* 61 (2016) 3964–3969.
- [62] I. Nezbeda, Vapour-liquid equilibria from molecular simulations: Some issues affecting reliability and reproducibility, *Mol. Phys.* 117 (2019) 2814–2821.
- [63] F.J. Wegner, Corrections to scaling laws, *Phys. Rev. B* 5 (1972) 4529–4536.
- [64] N.F. Carnahan, K.E. Starling, Equation of state for nonattracting rigid spheres, *J. Chem. Phys.* 51 (1969) 635–636.
- [65] A.L. Benavides, A. Gil-Villegas, The thermodynamics of molecules with discrete potentials, *Mol. Phys.* 97 (1999) 1225–1232.
- [66] J.A. Barker, D. Henderson, Perturbation theory and equation of state for fluids: The square-well potential, *J. Chem. Phys.* 47 (1967) 2856–2861.
- [67] J.A. Barker, D. Henderson, Perturbation theory and equation of state for fluids. II. A successful theory of liquids, *J. Chem. Phys.* 47 (1967) 4714–4721.
- [68] R. Espindola-Heredia, F. del Río, A. Malijevsky, Optimized equation of the state of the square-well fluid of variable range based on a fourth-order free-energy expansion, *J. Chem. Phys.* 130 (2009) 024509(1)–024509(13).
- [69] A.L. Benavides, F. del Río, Properties of the square-well fluid of variable width III. Long-range expansion, *Mol. Phys.* 68 (1989) 983–1000.
- [70] F. del Río, A.L. Benavides, Y. Guevara, Vapor-liquid equilibrium of a multipolar square-well fluid II. Effect of a variable square-well range, *Physica A* 215 (1995) 10–20.
- [71] G. Stell, J.C. Rasaiah, H. Narang, Thermodynamic perturbation theory for simple polar fluids. II, *Mol. Phys.* 27 (1974) 1393–1414.
- [72] S. Lago, B. Garzón, S. Calero, C. Vega, Accurate simulations of the vapor-liquid equilibrium of important organic solvents and other diatomics, *J. Phys. Chem. B* 101 (1997) 6763–6771.
- [73] B. Larsen, J.C. Rasaiah, G. Stell, Thermodynamic perturbation theory for multipolar and ionic liquids, *Mol. Phys.* 33 (1977) 987–1027.
- [74] S. Stephan, J. Staubach, H. Hasse, Review and comparison of equations of state for the lennard-jones fluid, *Fluid Phase Equilib.* 523 (2020) 112772(1)–112772(24).
- [75] R. Hentschke, J. Bartke, F. Pesth, Equilibrium polymerization and gas-liquid critical behavior in the stockmayer fluid, *Phys. Rev. E* 75 (2007) 011506(1)–011506(8).
- [76] J.A. White, Contribution of fluctuations to thermal properties of fluids with attractive forces of limited range: theory compared with $P\rho T$ and C_V , data for argon, *Fluid Phase Equilib.* 75 (1992) 53–64.
- [77] L.W. Salvino, J.A. White, Calculation of density fluctuation contributions to thermodynamic properties of simple fluids, *J. Chem. Phys.* 96 (1992) 4559–4568.